Check for updates

Received: 7 May 2026 | Accepted: 9 August 2026

DOI: 10.1111/aos.70220

Acta Ophthalmologica

ORIGINAL ARTICLE

Clinical and molecular features of *PRCD*-associated retinopathy

Vasil Kostin[1,2] | Karolina Kaminska[1,3] | Marco Cattaneo[3,4] | Enrico Ambrosini[5] | Carmen Ayuso[6,7] | Almudena Ávila-Fernández[6,7] | Béatrice Bocquet[8] | Luisa Coutinho-Santos[9] | Benedetto Falsini[10] | Lidia Fernandez-Caballero Palomeque[6,7] | Bohdan Kousal[11] | Petra Liskova[11,12] | Inmaculada Martín-Mérida[6,7] | María Juliana Ballesta-Martínez[13,14] | Daan Panneman[15] | Susanne Roosing[15] | Isabelle Meunier[8] | José M. Millán[16] | Monika Pankievič[12] | Irene Perea-Romero[6] | Virginie Peter[3] | Giorgio Placidi[10] | Cristina Santos[9,17] | Francesca Simonelli[18] | Ana Berta Sousa[19,20] | Francesco Testa[18] | Marie Vajter[11,12] | Marianna Weener[21] | Mathieu Quinodoz[1,3,22] | Carlo Rivolta[1,3,22] | Giacomo Calzetti[23,24]

Correspondence
Giacomo Calzetti, Vista Vision Eye Clinic, Borgo Pietro Wührer 129, Brescia 25123, Italy.
Email: giacomocalzetti@gmail.com

Abstract

Purpose: To describe the clinical and genetic characteristics of patients with biallelic disease-causing variants in the *PRCD* (Progressive Rod-Cone Degeneration) gene.

Methods: Multicentre, retrospective cohort study of 19 patients from 13 families across nine reference centres in six countries. Clinical assessments included best-corrected visual acuity (BCVA), kinetic visual field (VF), optical coherence tomography, and fundus autofluorescence (FAF). BCVA and VF area progression rates were estimated using linear mixed models on log-converted variables. Genetic testing was performed via Sanger sequencing, targeted gene panels, whole-exome sequencing, or whole-genome sequencing.

Results: Median age at symptom onset was 11 years, with nyctalopia as the main initial complaint. Mean age at low vision and legal blindness in the best-seeing eye was 35 and 38 years, respectively. BCVA declined at 0.046 logMAR/year (95% CI: 0.027–0.065; $p < 0.001$), corresponding to a 10.0% annual loss. VF area (V4e isopter) decreased by 19.4% annually. The time to reach the limit of significant change was <2 years for both BCVA and VF area. FAF showed a gradient from hyperautofluorescent arc in the youngest patient to extensive atrophy in older patients with advanced disease. Five distinct loss-of-function variants were identified, including two nonsense, two splice-site variants, and a whole-gene deletion.

Conclusion: Biallelic *PRCD* variants cause autosomal recessive retinitis pigmentosa, most often manifesting during childhood and showing relatively rapid progression of visual function loss. This information could prove useful for patient counselling and the planning of prospective natural history studies and targeted therapeutic approaches.

KEYWORDS
genetics, *PRCD*, progressive rod-cone degeneration, retinitis pigmentosa

For affiliations refer to page 10.

This is an open access article under the terms of the Creative Commons Attribution License, which permits use, distribution and reproduction in any medium, provided the original work is properly cited.
© 2026 The Author(s). *Acta Ophthalmologica* published by John Wiley & Sons Ltd on behalf of Acta Ophthalmologica Scandinavica Foundation.

1 | INTRODUCTION

Retinitis pigmentosa (RP) is the most common clinical form of inherited retinal disease (IRD) and encompasses a group of retinopathies characterized by rod vision loss and subsequent cone vision loss, often resulting in severe visual impairment. One of the genes implicated in autosomal recessive RP is *PRCD* (Progressive Rod-Cone Degeneration or Photoreceptor Disc Component), which encodes an exceptionally small protein consisting of 54 amino acids. The discovery and characterization of *PRCD* came largely from studies in canines affected by a form of inherited retinal degeneration. Genetic mapping in these dog breeds localized the disease locus close to the centromeric end of chromosome 9 (Acland et al., 1998), leading to the identification of the *Prcd* gene and a recurrent pathogenic variant p.(Cys2Tyr) (Zangerl et al., 2006), which was found to be the most common mutation across breeds. This is precisely the same variant that was identified in a homozygous state in a Bangladeshi woman affected with RP (Zangerl et al., 2006), making the canine model exceptionally relevant for translational research. Animal models have also been valuable for understanding the role of the gene in the retina. In the murine retina, *Prcd* is expressed as early as embryonic Day 14, and localizes to photoreceptor outer segments (Allon et al., 2019). Immunoelectron microscopy has revealed that the protein is not distributed throughout the outer segment but is concentrated at specific locations: the outer segment disc rim and, notably, at the base of the outer segment where disc formation occurs. $Prcd^{-/-}$ mice develop progressive retinal degeneration starting at 20 weeks of age, with a significant reduction in both scotopic and photopic electroretinographic responses (Allon et al., 2019). These mice show accumulation of extracellular vesicles in the interphotoreceptor matrix and severe damage to photoreceptor outer segments (Allon et al., 2019; Spencer et al., 2019). Interestingly, phagocytosis of shed outer segment discs by the retinal pigment epithelium (RPE) is reduced in $Prcd^{-/-}$ mice, suggesting a role in coordinating disc formation, shedding, and phagocytosis. Furthermore, in $Prcd^{-/-}$ mice, retinal lipid dysregulation was observed, including altered cholesterol and phospholipid levels, with upregulation of the ABCA1 transporter in the RPE (Motipally et al., 2024). These mice also develop drusen and subretinal drusenoid-like deposits—hallmarks of age-related macular degeneration (Motipally et al., 2024). In canine models, the deficiency leads to progressive retinal degeneration characterized by lamellar disorientation and vesicular profiles in the outer segments (Aguirre et al., 1982). Optical coherence tomography (OCT) studies in mutant dogs demonstrate significant thinning of the outer retina (Dufour et al., 2026; Park et al., 2022). Despite extensive characterization of animal models, knowledge about human retinopathy due to biallelic disease-causing variants in *PRCD* is limited (Dufour et al., 2026; Fu et al., 2013; Nevet et al., 2010; Pach et al., 2013; Peng et al., 2025; Remez et al., 2014; Zangerl et al., 2006). The purpose of this study was to define the clinical phenotype and molecular spectrum of PRCD-associated human retinopathy in a multicentre international cohort.

2 | METHODS

2.1 | Patients

This observational cohort study included patients with biallelic pathogenic or likely pathogenic variants in the *PRCD* gene who were examined at nine reference centres for IRDs in six countries: Czech Republic (1 patient), France (1 patient), Italy (3 patients, 2 families), Portugal (1 patient), Russia (1 patient), and Spain (12 patients, 7 families). Medical records were reviewed to retrieve data on family and medical history, best-corrected visual acuity (BCVA) measured using Early Treatment Diabetic Retinopathy Study (ETDRS) charts or Snellen charts, slit lamp biomicroscopy (in particular, presence of cataract or other pathologies that could affect visual function), fundus examination, kinetic visual field (VF) as assessed with Goldmann perimeter using the V4e target, OCT, fundus autofluorescence (FAF) and full-field electroretinography (ERG) performed in accordance with International Society for Clinical Electrophysiology of Vision standards. Informed consent was obtained from the subjects after explanation of the nature and possible consequences of the study, and the research was conducted in compliance with the ethics committees of the involved centres and in accordance with the Declaration of Helsinki.

2.2 | BCVA and VF analysis

BCVA was converted to the logarithm of the minimum angle of resolution (logMAR) equivalent for statistical analysis. Visual acuities of counting fingers, hand motion, light perception, and no light perception were assigned values of 2.1, 2.4, 2.7, and 3.0 logMAR, respectively (Day et al., 2015). VF examinations were performed using the V4e target. For quantitative analysis, we employed a digital method to quantify Goldmann VF data using Adobe Photoshop (v.26.2.020241202.m.2890), following the previously described methodology (Zahid et al., 2014). Briefly, paper Goldmann VF charts were scanned at high resolution (300 dpi) and imported into Adobe Photoshop. The boundaries of the V4e isopter were manually traced using the selection tool, and the enclosed area was filled with a distinct colour. The number of pixels within the selected area was then quantified using the histogram function in Photoshop and converted to square degrees. VF digitalization and subsequent Photoshop analysis were performed by author V.K.

2.3 | Retinal imaging

OCT was performed using the Spectralis (Heidelberg Engineering, Germany), the Cirrus HD-OCT (Carl Zeiss Meditec, USA) or the DRI OCT Triton Plus (Topcon, Japan). FAF was short-wavelength (performed with the Spectralis), except for the Portuguese patient who had mid-wavelength FAF performed with the DRI OCT Triton Plus.

17553768, 0, Downloaded from https://onlinelibrary.wiley.com/doi/10.1111/aos.70220 by Servicio Murciano De Salud, Wiley Online Library on [27/10/2026]. See the Terms and Conditions (https://onlinelibrary.wiley.com/terms-and-conditions) on Wiley Online Library for rules of use; OA articles are governed by the applicable Creative Commons License

2.4 | Molecular testing

Genomic DNA was extracted from peripheral blood or saliva samples according to standard protocols. Genetic testing across contributing centres was performed via Sanger sequencing of *PRCD*, targeted gene panels, whole-exome sequencing, or whole-genome sequencing, as available at the time of the diagnosis. All variants were validated using VariantValidator (Freeman et al., 2018), described in accordance with the Human Genome Variation Society nomenclature (den Dunnen et al., 2016), and classified based on the criteria of the American College of Medical Genetics and Genomics (Richards et al., 2015). Frequencies of variants in the general population were obtained from the gnomAD database (Karczewski et al., 2020). Each variant was cross-checked in the ClinVar repository (Landrum et al., 2016), and biomedical literature. For the intronic variants, predicted effects on splicing were assessed using SpliceAI (Jaganathan et al., 2019).

2.5 | Statistical analysis

The annual rates of change of BCVA and V4e VF area were based on linear mixed models with age as fixed effect and patient and eye as nested random intercepts. Both cross-sectional and longitudinal data were included in the analysis. The model assumptions were checked graphically and appeared reasonable. Inclusion of random slopes or centre as additional nested random effect did not improve the model fit. VF area was $\log_{10}$-converted before calculation. The annual rates of change were expressed as a % by back-conversion of log-converted variables to the original scale. The time to reach the limit of significant change was derived as the quotient between the 95% repeatability coefficient divided by the rate of change. The 95% repeatability coefficients were taken from previous RP studies: ±0.078 [logMAR] and ±0.183 [$\log_{10}$] for BCVA and VF area, respectively (Berson et al., 1985; Roman et al., 2013).

The mean age at which low vision or legal blindness was reached in the best-seeing eye was calculated using >0.52 logMAR and ≥1.0 logMAR as thresholds for low vision and legal blindness, respectively. The Pearson correlation coefficient between the values of the two eyes of a patient was used to test interocular symmetry of BCVA and VF area.

All statistical analyses were conducted with the statistical software package R version 4.4.3, using 'two-sided' statistical tests and confidence intervals (with 5% significance and 95% confidence levels, respectively). Missing data were handled by available-case analyses. No correction for multiple testing was applied: p values and confidence intervals must be interpreted with care.

3 | RESULTS

3.1 | Patient cohort characterization

We studied 19 patients with genetically confirmed *PRCD*-associated retinopathy from 13 families. The familial clustering observed in our cohort, with multiple affected members in families and documented consanguinity in a subset of seven families, is consistent with the established autosomal recessive inheritance pattern of the disease. The cohort included 8 females and 11 males. Age at baseline examination ranged from 9 to 51 years. Demographics and baseline clinical characteristics are given in Table 1.

Clinical diagnosis was non-syndromic RP in all patients. In the 17 patients with documented age at symptom onset, this ranged between <5 and 25 years (median: 11 years), with 9 (53%) experiencing childhood-onset disease (≤11 years), 3 (18%) presenting during adolescence (12–18 years), and 5 (29%) developing symptoms in adulthood (>18 years). The main initial symptom was decreased night vision in all these patients. Rod and cone ERG data were available in 6 patients (P1 at age 28, P8 at age 69, P10 at age 50, P13 at age 32, P14 at age 37, and P15 at age 34): these patients had no detectable responses to any stimuli.

3.2 | BCVA progression

To characterize the natural history of BCVA loss we analysed 15 patients with documented measurements. Four patients had serial data: P1 (3 visits spanning 13 years from age 28 to age 41), P8 (2 visits spanning 29 years from age 40 to age 69), P9 (2 visits spanning 4 years from age 49 to age 53), and P10 (2 visits spanning 6 years from age 50 to age 56). A significant correlation was found between age and BCVA (β=0.046; 95% confidence interval=0.027, 0.065; p<0.001), with an average deterioration of 0.046 logMAR/year, corresponding to losing each year 10.0% of the residual BCVA (Figure 1). The time to reach the limit of significant change was 1.70 years. The mean age for reaching critical visual thresholds of low vision and legal blindness in the best-seeing eye was 34.7 (95% prediction interval=14.7, 54.8) and 38.0 (95% prediction interval=18.1, 57.8), respectively. As there were three predominant homozygous disease-causing variants (c.64C>T, N=5; c.102_111dup, N=4; c.74+1G>A, N=4), we asked whether there was an effect of the variant on BCVA progression: no clear effect was found (p=0.31).

3.3 | VF area progression

VFs from four patients were available. One of these patients had serial examinations spanning 9 years (P1, five examinations from age 28 to age 37), which revealed isopter constriction with disease progression. Two patients in the fifth decade displayed severely constricted fields with a central island ≤20° in diameter, while one patient aged 40 maintained residual inferior-temporal crescents (Figure 2). A significant correlation was found between age and VF area (β=−0.093; 95% confidence interval=−0.111, −0.076; p<0.001). The yearly progression of $\log_{10}$(square degrees) was 0.093, corresponding to losing 19.4% of the residual VF area each year. The time to reach the limit of significant change was 1.96 years (Figure 3).

17553768, 0, Downloaded from https://onlinelibrary.wiley.com/doi/10.1111/aos.70220 by Servicio Murciano De Salud, Wiley Online Library on [27/10/2026]. See the Terms and Conditions (https://onlinelibrary.wiley.com/terms-and-conditions) on Wiley Online Library for rules of use; OA articles are governed by the applicable Creative Commons License

TABLE 1 Molecular, demographic, and baseline clinical characteristics of patients with *PRCD* variants.

		Disease-causing variant(s)								BCVA (Snellen fraction) at baseline
Family ID	Patient ID	Nucleotide change	Amino acid change or predicted effect	Zygosity	Country	Sex	Clinical diagnosis	Age at onset of symptoms	Age at baseline	OD–OS
F1	P1	c.64C>T	p.(Arg22Ter)	Hom	France (Algerian origin)	F	RP	8	28	20/50–20/40
F2	P2	c.64C>T	p.(Arg22Ter)	Hom	Russia (Azerbaijani origin)	F	RP	9	34	20/100–20/640
F3	P3	c.64C>T	p.(Arg22Ter)	Hom	Spain	M	RP	NA	38	20/50–20/32
F4	P4	c.64C>T	p.(Arg22Ter)	Hom	Spain	M	RP	20	43	HM - HM
F5	P5	c.64C>T	p.(Arg22Ter)	Hom	Spain	F	RP	7	NA	NA
F6	P6	c.64C>T	p.(Arg22Ter)	Hom	Spain	M	RP	11	24	20/50–20/50
F6	P7	c.64C>T	p.(Arg22Ter)	Hom	Spain	M	RP	NA	NA	NA
F7	P8	c.102_111dup	p.(Ser38Ter)	Hom	Italy	F	RP	6	40	20/500–20/500
F8	P9	c.102_111dup	p.(Ser38Ter)	Hom	Italy	F	RP	25	49	20/80–20/125
F8	P10	c.102_111dup	p.(Ser38Ter)	Hom	Italy	M	RP	13	50	20/20–20/40
F9	P11[a]	c.102_111dup	p.(Ser38Ter)	Hom	Portugal	M	RP	21	51	LP - LP
F10	P12[b]	(1) c.102_111dup (2) c.74+5G>C	(1) p.(Ser38Ter) (2) p.?	Comp het	Spain	M	RP	12	27	LP - LP
F11	P13	c.74+1G>A	p.?	Hom	Spain	F	RP	21	32	20/25–20/25
F11	P14	c.74+1G>A	p.?	Hom	Spain	M	RP	25	37	20/50–20/50
F11	P15	c.74+1G>A	p.?	Hom	Spain	M	RP	16	46	HM - LP
F12	P16	c.74+1G>A	p.?	Hom	Spain	F	RP	<5	26	20/20–20/80
F12	P17	c.74+1G>A	p.?	Hom	Spain	F	RP	8	NA	NA
F12	P18	c.74+1G>A	p.?	Hom	Spain	M	RP	5	NA	NA
F13	P19	Deletion of the whole *PRCD* gene		Hom	Czech Republic (Slovakian origin)	M	RP	6	9	20/32–20/32

Abbreviations: BCVA, best-corrected visual acuity; Comp het, compound heterozygous; HM, hand motion; Hom, homozygous; LP, light perception; NA, not available; OD, right eye; OS, left eye; RP, retinitis pigmentosa.

[a]Molecular results were published (Peter et al., 2023), and submitted to ClinVar.

[b]Segregation analysis confirmed the variants are on separate alleles (*in trans*).

17553768, 0, Downloaded from https://onlinelibrary.wiley.com/doi/10.1111/aos.70220 by Servicio Murciano De Salud, Wiley Online Library on [27/10/2026]. See the Terms and Conditions (https://onlinelibrary.wiley.com/terms-and-conditions) on Wiley Online Library for rules of use; OA articles are governed by the applicable Creative Commons License

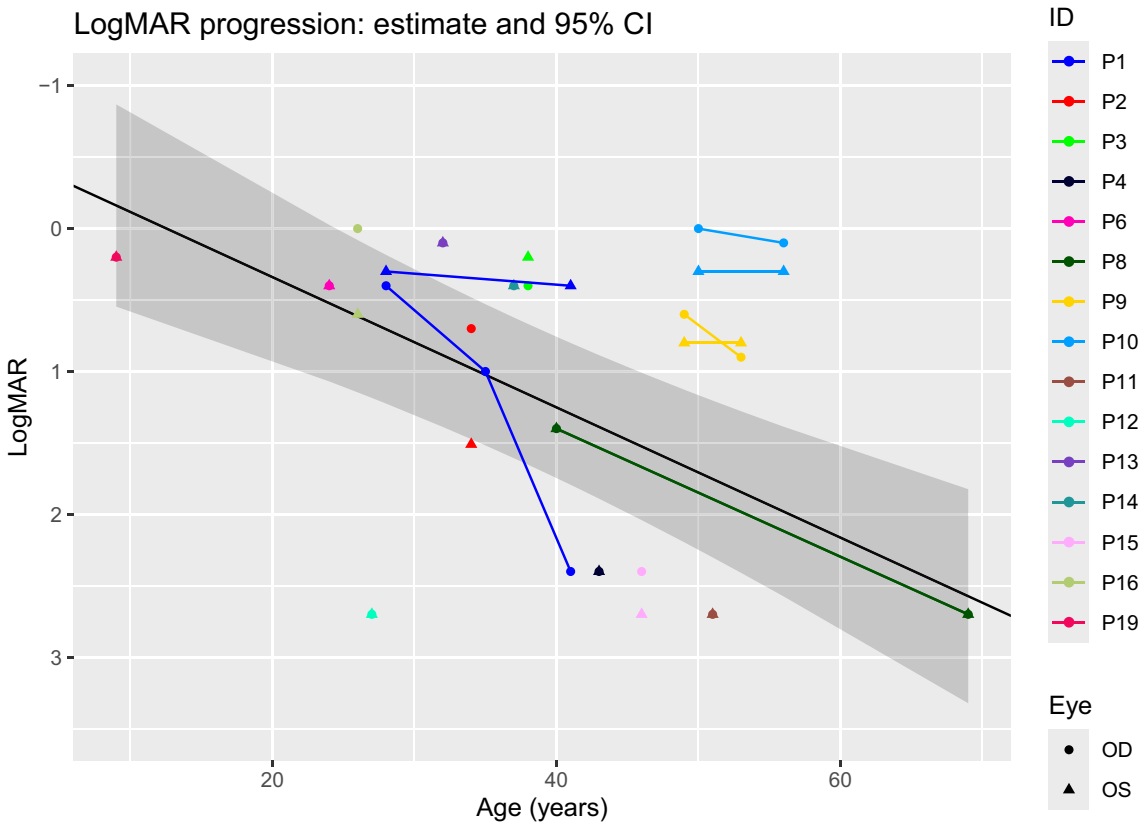

FIGURE 1 Visual acuity as a function of age in *PRCD* patients. Solid lines connect serial data of the same eye. The solid black line is the mean rate of visual acuity loss, while the grey shaded area represents the 95% confidence interval. Colour key for the patients, on the right.

3.4 | Disease symmetry between eyes

Symmetry analysis between right and left eyes demonstrated a strong correlation for both BCVA ($r=0.87$, $p<0.001$) and VF area ($r=0.85$, $p=0.028$), suggesting that the disease affects both eyes similarly, though some interocular asymmetry was present in a subset of patients. The mean interocular difference in BCVA was 0.167±0.249 logMAR.

3.5 | Retinal imaging

OCT and FAF were available in eight patients (6 patients had both, 1 only OCT, 1 only FAF), as displayed in Figure 4. The youngest patient (P19, aged 9 years) had relatively intact retinal lamination, though a subtle hyperreflective alteration was noted within the outer nuclear layer at the fovea in both eyes, together with an abnormal thinning of the outer nuclear layer with increasing eccentricity from the fovea. FAF showed a hyperautofluorescent arc in the right eye, and fundus examination revealed bone spicule-like pigment deposits in the periphery of both eyes.

At age 33, P12 showed pigment deposits in the periphery and macular atrophy.

Likewise, P1 at the age of 41 presented with complete RPE and outer retinal atrophy; partial foveal sparing in the left eye accounted for the interocular asymmetry in BCVA.

P9 and P10 were siblings aged 49 and 50. Their FAF showed a relatively spared macular RPE surrounded by hypoautofluorescence. The left foveola of P9 had RPE atrophy. Cystoid macular oedema (CME) was present in both eyes of P10. This patient was treated with oral acetazolamide, which improved the CME. However, he experienced dizziness and had renal colic while on treatment, and the medication was discontinued. Six years later, the patient still had CME but, fortunately, only a slight decline in visual acuity (decreased from 20/20 to 20/25 in the right eye and remained at 20/40 in the left eye). Fundus examination of both P9 and P10 showed bone spicule-like pigment deposits in the periphery, attenuated retinal vessels with focal arteriolar sheathing, and optic nerve head drusen.

The two oldest patients with available images (P11 aged 51 and P8 aged 76) presented an advanced disease with extensive RPE atrophy and subtotal loss of outer retinal layers.

Review of the clinical records did not reveal any clinical suspicion of CME in the patients without OCT scans, and none of these patients received carbonic anhydrase inhibitors.

3.6 | Molecular diagnosis

All of the patients in this cohort carried rare biallelic loss-of-function (LoF) variants in *PRCD*, with the majority found in a homozygous state and one case of compound heterozygosity (Table 1). Two of the variants were nonsense mutations (M1 and M2), two were predicted to affect mRNA splicing (M3 and M4), and one was a large genomic deletion (M5) spanning the entire *PRCD* coding region (Figure 5).

17553768, 0, Downloaded from https://onlinelibrary.wiley.com/doi/10.1111/aos.70220 by Servicio Murciano De Salud, Wiley Online Library on [27/10/2026]. See the Terms and Conditions (https://onlinelibrary.wiley.com/terms-and-conditions) on Wiley Online Library for rules of use; OA articles are governed by the applicable Creative Commons License

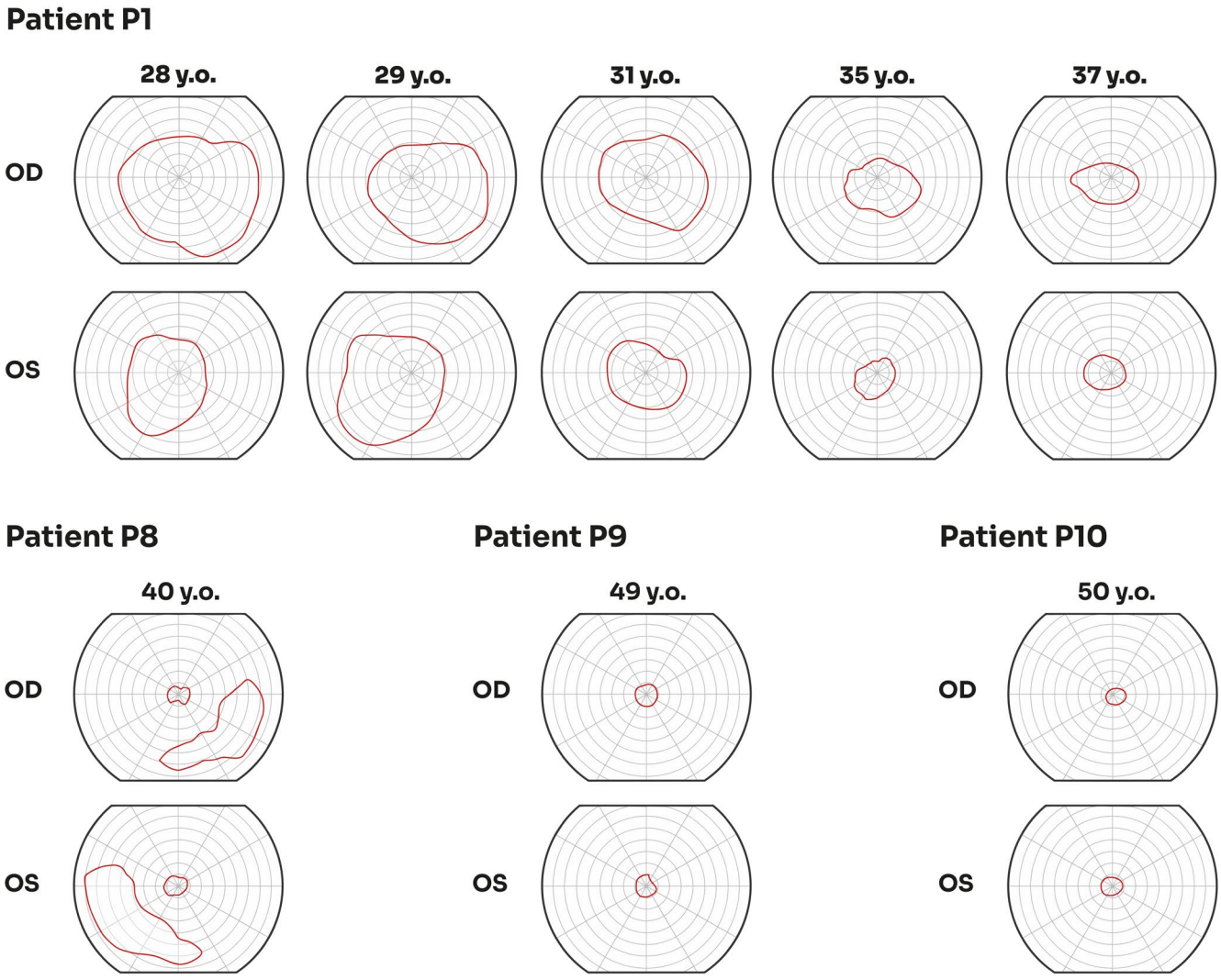

FIGURE 2 Kinetic perimetry in *PRCD* patients. Serial visual fields of patient P1 and individual visual fields of patients P8, P9, and P10 are shown, along with the patient age when the data were collected. The V4e test target is shown.

The most recurrent variant, M1 [NM_001077620.3:c.64C>T, p.(Arg22Ter)], was identified in a homozygous state in seven patients from six independent families across Spain, France, and Russia. This variant has been previously reported in ClinVar as pathogenic, initially described as a founder mutation in an Israeli Muslim Arab subpopulation, and subsequently observed in patients of diverse national backgrounds (Table S1) (Koyanagi et al., 2019; Nevet et al., 2010; Perez-Carro et al., 2016). The second most frequent variant, M2 [c.102_111dup, p.(Ser38Ter)], was found in five patients from four unrelated families from Italy, Spain, and Portugal. Although previously reported in ClinVar with conflicting interpretations (likely pathogenic and variant of uncertain significance, VUS), this duplication introduces a premature termination codon in exon 2 and is predicted to trigger nonsense-mediated mRNA decay. In one patient, it was identified *in trans* with M3 (c.74+5G>C, p.?), variant, classified as a VUS in ClinVar and previously reported in literature in one individual with RP (Rodríguez-Muñoz et al., 2020). SpliceAI predicts that this change disrupts the canonical donor splice site (delta score: 0.96, out of 1.00), while a new donor site 29 bp upstream shows a gain score of 0.19. This is predicted to result in either the skipping of exon 2 or the inclusion of an additional 29 bp, leading to a frameshift and a premature termination codon. A similar effect is predicted for M4 (c.74+1G>A, p.?), identified in a homozygous state in six affected individuals from two Spanish families. This variant has been previously classified as likely pathogenic/pathogenic for *PRCD*-associated RP (Perez-Carro et al., 2016). Lastly, one patient carried a large homozygous genomic deletion with a 5-base pair microhomology at the breakpoint (M5, NC_000017.10:g.74528309_74540884del), encompassing the entire coding part of *PRCD*, as well as the first coding exon of a nearby gene, *CYGB* (NM_134268.5). A similar event has been previously reported as pathogenic in ClinVar (ID: 3243136), although the precise genomic coordinates were not established, preventing confirmation of identity.

4 | DISCUSSION

Biallelic disease-causing *PRCD* variants cause a retinopathy that most often manifests during childhood and leads to low vision in the best-seeing eye by an average age of 34.7 years.

We have estimated annual rates of visual function loss: the 10.0% annual rate of visual acuity loss indicates

17553768, 0, Downloaded from https://onlinelibrary.wiley.com/doi/10.1111/aos.70220 by Servicio Murciano De Salud, Wiley Online Library on [27/10/2026]. See the Terms and Conditions (https://onlinelibrary.wiley.com/terms-and-conditions) on Wiley Online Library for rules of use; OA articles are governed by the applicable Creative Commons License

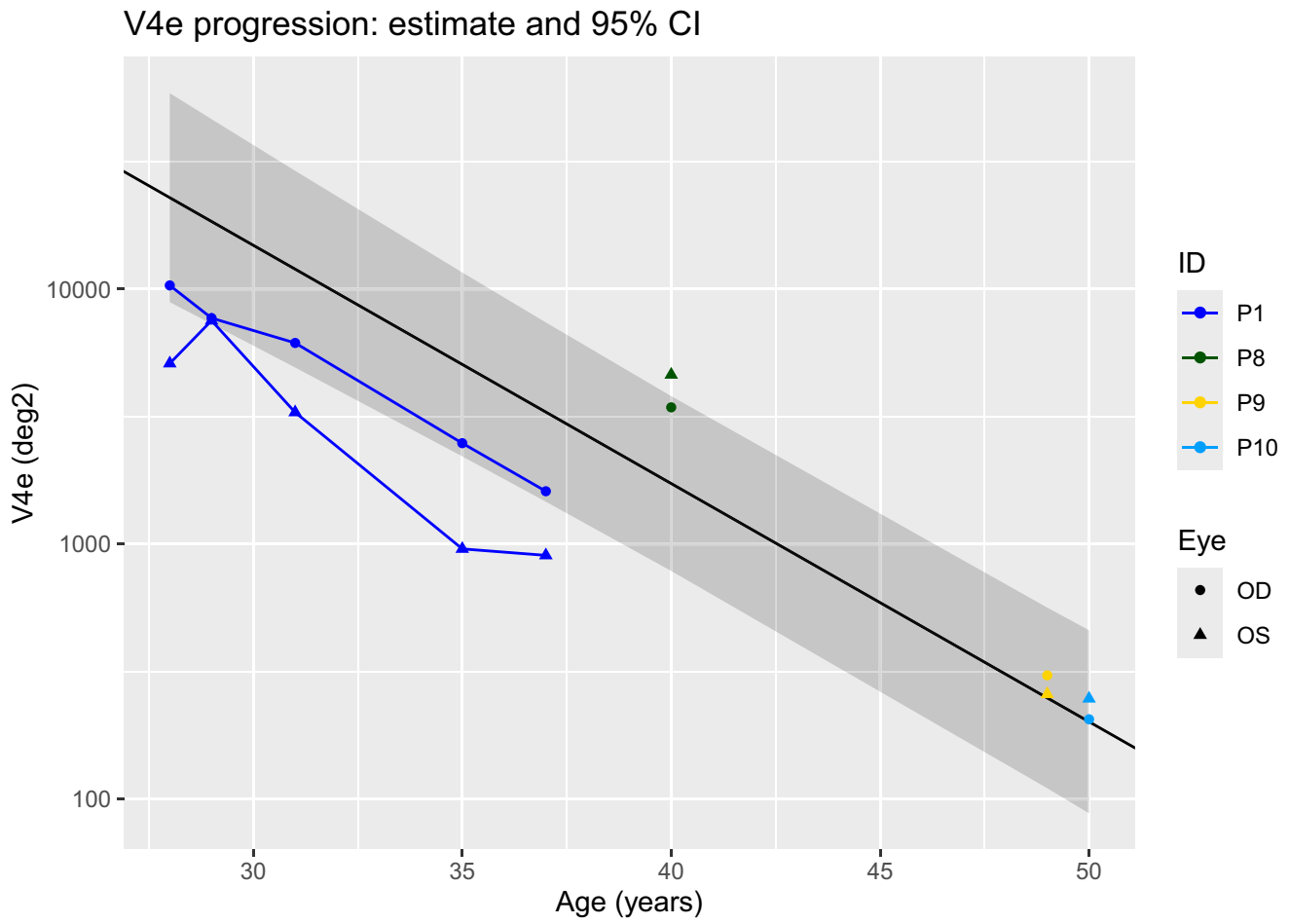

FIGURE 3 Visual field area to the V4e target as a function of age in *PRCD* patients. Solid lines connect serial data of the same eye. The solid black line is the mean rate of visual field loss, while the grey shaded area represents the 95% confidence interval. Colour key for the patients, on the right.

faster progression than other common RP genotypes. For example, a rate of 2.5%/year was found for *USH2A* caused by the c.2299del mutation (Calzetti et al., 2018), 5.7%/year for *EYS* (McGuigan et al., 2017), and 8.2%/year for *RPGR Orf15* mutations (Huang et al., 2012). Our findings are consistent with previous reports of *PRCD*-associated retinopathy, showing that maculopathy is a frequent feature. It seems that some patients developed, in addition to generalized dystrophy, a more macular-affecting phenotype with geographic atrophy (e.g., P1 and P12), whereas others presented with a more typical RP type of a disease where macular RPE is rather spared (e.g., P10). So there seems to be some variation in macular phenotype without obvious correlation to genotype nor age. Interestingly, drusen and subretinal drusenoid deposits (SDD)-like focal deposits in addition to extensive lipofuscin accumulation were found in $Prcd^{-/-}$ mice, indicating an age-related macular degeneration (AMD)-like phenotype (Motipally et al., 2024). Although we could not identify drusen or SDD-like deposits in our patients, some mechanisms that cause the AMD-like phenotype in mice might also be present in the PRCD-deficient human retina and contribute to the maculopathy. Further studies involving a larger number of patients could clarify whether drusen and SDD-like deposits are present at different stages of the disease. It is noteworthy, however, that while all patients over the age of 30 described previously had visual acuity of less than 20/70 in their best-seeing eye, we have shown that it is possible to maintain visual acuity of 20/25 up to the age of 56. With regard to the kinetic VF area loss, we measured an annual rate of 19.4%, which falls between the 9.4% of *USH2A* c.2299delG and the 23.1% of *EYS* (Calzetti et al., 2018; McGuigan et al., 2017).

To date, only 14 variants in *PRCD* have been reported as pathogenic, underscoring the recurrence of genotypes and the presence of independent founder effects. This pattern is mirrored in our cohort, where we identified five distinct *PRCD* variants across 19 individuals from 13 unrelated families. The majority of reported disease-causing variants represent LoF alleles, with only two missense changes classified as pathogenic. Consistent with this, all patients in our study carried biallelic LoF mutations. Although larger studies are needed to assess the impact of specific mutations on the phenotype, we found no significant correlation between three prevalent homozygous mutations and visual acuity progression, which is consistent with all the homozygous mutations analysed being LoF.

The limitations of the study lie in its retrospective design, small sample size, and lack of relevant tests, such as full-field stimulus testing. In addition, retinal

17553768, 0, Downloaded from https://onlinelibrary.wiley.com/doi/10.1111/aos.70220 by Servicio Murciano De Salud, Wiley Online Library on [27/10/2026]. See the Terms and Conditions (https://onlinelibrary.wiley.com/terms-and-conditions) on Wiley Online Library for rules of use; OA articles are governed by the applicable Creative Commons License

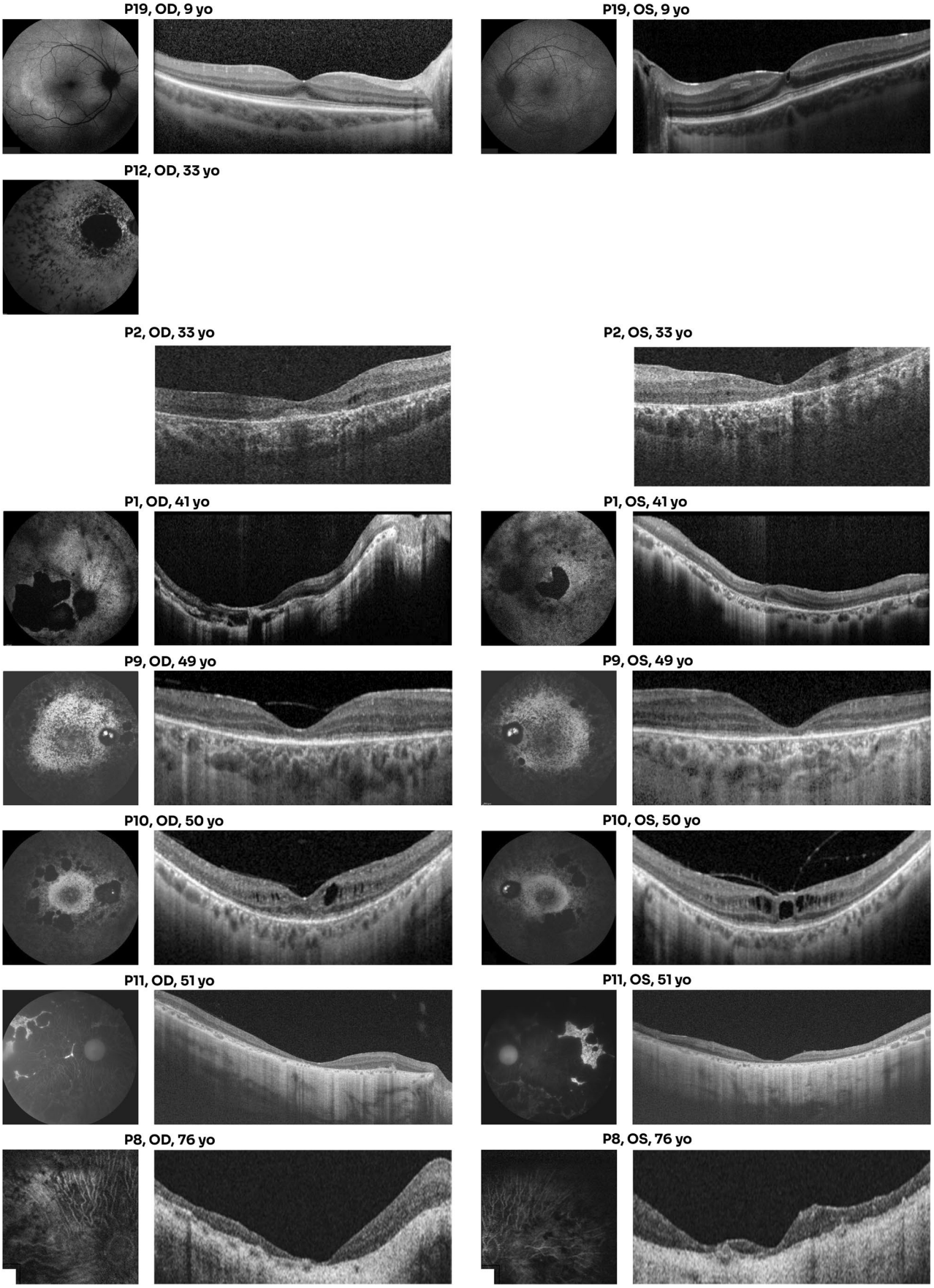

FIGURE 4 Multimodal retinal imaging of *PRCD* patients. Each row displays, from left to right, the fundus autofluorescence (FAF) of the right eye, the optical coherence tomography (OCT) of the right eye, the FAF of the left eye, and the OCT of the left eye. Patients are listed from top to bottom based on the age at which the examinations were performed. OCT images are scans passing through the fovea.

17553768, 0, Downloaded from https://onlinelibrary.wiley.com/doi/10.1111/aos.70220 by Servicio Murciano De Salud, Wiley Online Library on [27/10/2026]. See the Terms and Conditions (https://onlinelibrary.wiley.com/terms-and-conditions) on Wiley Online Library for rules of use; OA articles are governed by the applicable Creative Commons License

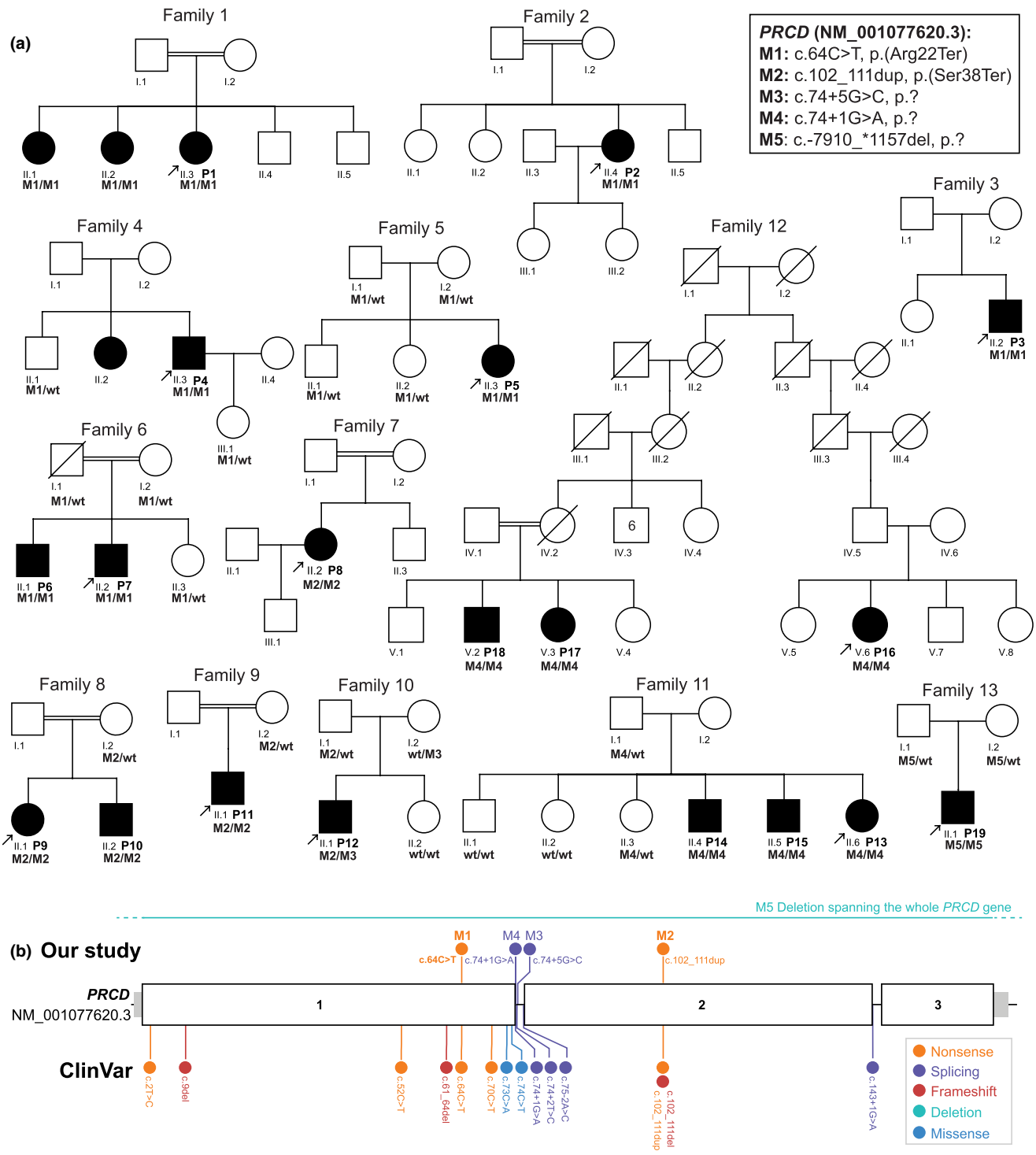

FIGURE 5 Pedigrees of the analysed individuals (a) and schematic representation of the mutational spectrum of *PRCD* variants (b). (a) Probands from every family are indicated by arrows. White and black shapes denote healthy and affected individuals, respectively; squares = males; circles = females; symbols with a diagonal line = deceased; double horizontal lines = consanguineous union. Clinical data were available for 19 individuals (P1–P19) from 13 families. Disease-associated variants are indicated by MX (M1–M5), with their detailed notation listed in the table, while 'wt' denotes the wild-type allele. (b) Schematic representation of the *PRCD* gene (based on the canonical transcript, NM_001077620.3) showing the location of variants identified in this study (above), and pathogenic/likely pathogenic variants reported in the ClinVar database (below). Exons are depicted as numbered boxes and introns as horizontal lines (not at scale). Untranslated regions (UTRs) are shown in grey. Variant types are colour-coded as indicated. M5, a large deletion spanning the entire coding sequence of *PRCD*, is indicated by a horizontal line.

imaging and ERG were not available in all patients. It is significant that all patients presented with night blindness, a rod-mediated symptom, as their initial complaint. However, all available ERG responses were non-detectable for both rod- and cone-mediated components at the time of testing (from age 28 onward); therefore, our ERG data cannot establish the timing of rod versus cone photoreceptor involvement early in the disease course. Nonetheless, this study represents, to the best of our knowledge, the largest clinically and molecularly characterized cohort of *PRCD*-associated retinopathy reported to date and provides information

17553768, 0, Downloaded from https://onlinelibrary.wiley.com/doi/10.1111/aos.70220 by Servicio Murciano De Salud, Wiley Online Library on [27/10/2026]. See the Terms and Conditions (https://onlinelibrary.wiley.com/terms-and-conditions) on Wiley Online Library for rules of use; OA articles are governed by the applicable Creative Commons License

relevant to prognosis and future natural history study design.

PRCD is not a common cause of IRD. This observation is supported by analyses of large-scale genomic and patient databases (Branham et al., 2025; Hanany et al., 2020). In the gene poll conducted by the Foundation Fighting Blindness Clinical Consortium, this condition accounted for 0.04% of all patients with IRDs (Branham et al., 2025). However, the disease has been reported across diverse geographic backgrounds (Koyanagi et al., 2019; Midgley et al., 2024), and appears to be more prevalent in the Mediterranean basin, an area home to some populations that may have been genetically understudied. In anticipation of a clinical trial of therapy, the rarity of the disease certainly poses a hurdle, for example, to the development and commercial viability of a gene-specific therapeutic programme. On the other hand, certain factors would make *PRCD* an ideal candidate for the development of a gene-specific therapy product. First, the availability of a canine model that could be used for preclinical studies: the canine progressive rod-cone degeneration, due to a mutant *Prcd* allele shared by at least 65 dog breeds, has been extensively characterized over the past 50 years and represents one of the most studied large animal models of human RP. In canine progressive rod-cone degeneration, the rate of photoreceptor loss is greater for rods than for cones, and it initially occurs at the posterior pole rather than in the retinal periphery (Aguirre et al., 1982). However, in 5-year-old animals, the retina is best preserved in the posterior pole where only cone photoreceptors remain. Even though abnormalities in retinal function are usually present by 6 months to 1 year, clinical disease is not apparent until early adulthood (between 3 and 6 years old) (Aguirre et al., 1997). Despite potential similarities, it is important to bear in mind the difference between the human fovea and the canine fovea-like region, which could limit the translatability of animal study results. Second, the gene is particularly small, comprising a coding sequence of 162 bp, which is advantageous for insertion into adeno-associated viral vectors. Third, the rapid progression of the disease, which would make a clinical trial feasible over a shorter timeframe. In this regard, we found that the time to reach the limit of significant change was less than 2 years for both visual acuity and VF area.

In conclusion, we present the largest cohort of clinically and molecularly characterized *PRCD*-associated retinopathy. The disease is characterized by a generalized dystrophy with night blindness as the first complaint, most often manifesting during childhood. Progression of visual function loss is relatively rapid compared with other common RP genotypes. In addition, we report causative variations that broaden the mutational spectrum of *PRCD* and strengthen data currently available in genomic databases and biomedical literature. These findings could prove useful for patient prognosis, future development of natural history studies, and the design of targeted therapeutic approaches.

ACKNOWLEDGEMENTS

Carmen Ayuso and Lidia Fernandez-Caballero Palomeque acknowledge grants from the Instituto de Salud Carlos III (ISCIII) [PI22/00321, PI25/00246, and IMP/00009], Centro de Investigación Biomédica en Red Enfermedades Raras (CIBERER, 06/07/0036), the IIS-FJD BioBank (PT23/00114), the European Regional Development Fund (FEDER), the Organización Nacional de Ciegos Españoles (ONCE), and the University Chair UAM-IIS-FJD of Genomic Medicine. Benedetto Falsini acknowledges funding from ERN-EYE. Petra Liskova acknowledges funding from Ministry of Health of the Czech Republic (NW24-06-00083) and by institutional programs of Charles University in Prague UNCE/24/MED/022 and SVV 2600631. Open access publishing facilitated by Aziende Socio Sanitarie Territoriale Melegnano e della Martesana, as part of the Wiley – SBBL agreement. [Correction added on 23 September 2026, after first online publication: The acknowledgments section has been updated.]

AFFILIATIONS

[1]Department of Ophthalmology, University of Basel, Basel, Switzerland
[2]Nuffield Laboratory of Ophthalmology, Nuffield Department of Clinical Neurosciences, University of Oxford, Oxford, UK
[3]Institute of Molecular and Clinical Ophthalmology Basel, Basel, Switzerland
[4]Department of Clinical Research, University of Basel, Basel, Switzerland
[5]Medical Genetics, University Hospital of Parma, Parma, Italy
[6]Department of Genetics & Genomics, Instituto de Investigación Sanitaria-Fundación Jiménez Díaz University Hospital, Universidad Autónoma de Madrid (IIS-FJD, UAM), Madrid, Spain
[7]Centre for Biomedical Network Research on Rare Diseases (CIBERER), Instituto de Salud Carlos III, Madrid, Spain
[8]Institute for Neurosciences of Montpellier (INM), University of Montpellier, INSERM, Montpellier, France
[9]Instituto de Oftalmologia Dr. Gama Pinto, Unidade Local de Saúde (ULS) São José, E.P.E., Lisbon, Portugal
[10]Ophthalmology Unit, Fondazione Policlinico Universitario "A. Gemelli" IRCCS/Università Cattolica del S. Cuore, Rome, Italy
[11]Department of Ophthalmology, First Faculty of Medicine, Charles University and General University Hospital in Prague, Prague, Czech Republic
[12]Department of Paediatrics and Inherited Metabolic Disorders, First Faculty of Medicine, Charles University and General University Hospital in Prague, Prague, Czech Republic
[13]Sección de Genética Médica, Hospital Clínico Universitario Virgen de la Arrixaca, Murcia, Spain
[14]Instituto Murciano de Investigación Biosanitaria (IMIB), Murcia, Spain
[15]Department of Human Genetics, Radboud University Medical Center, Nijmegen, The Netherlands
[16]Instituto de Investigación Sanitaria La Fe (IIS La Fe) and CIBERER, Valencia, Spain
[17]iNOVA4Health, NOVA Medical School, Faculdade de Ciências Médicas, NMS, FCM, Universidade NOVA de Lisboa, Lisbon, Portugal

17553768, 0, Downloaded from https://onlinelibrary.wiley.com/doi/10.1111/aos.70220 by Servicio Murciano De Salud, Wiley Online Library on [27/10/2026]. See the Terms and Conditions (https://onlinelibrary.wiley.com/terms-and-conditions) on Wiley Online Library for rules of use; OA articles are governed by the applicable Creative Commons License

[18]Eye Clinic, Multidisciplinary Department of Medical, Surgical and Dental Sciences, University of Campania "Luigi Vanvitelli", Naples, Italy
[19]Department of Medical Genetics, ULS St Maria, Lisbon, Portugal
[20]Clínica Universitária de Genética Médica, Faculty of Medicine, University of Lisbon, Lisbon, Portugal
[21]Mass Eye and Ear, Ocular Genomics Institute, Harvard Medical School, Boston, Massachusetts, USA
[22]Department of Genetics, Genomics and Cancer Sciences, University of Leicester, Leicester, UK
[23]Vista Vision Eye Clinic, Brescia, Italy
[24]ASST Melegnano Martesana, Milan, Italy

ORCID

Marco Cattaneo https://orcid.org/0000-0002-6610-8431
Petra Liskova https://orcid.org/0000-0001-7834-8486
Marianna Weener https://orcid.org/0000-0002-1089-4293
Carlo Rivolta https://orcid.org/0000-0002-0733-9950
Giacomo Calzetti https://orcid.org/0000-0003-1391-9510

REFERENCES

Acland, G.M., Ray, K., Mellersh, C.S., Gu, W., Langston, A.A., Rine, J. et al. (1998) Linkage analysis and comparative mapping of canine progressive rod-cone degeneration (prcd) establishes potential locus homology with retinitis pigmentosa (RP17) in humans. *Proceedings of the National Academy of Sciences of the United States of America*, 95(6), 3048–3053.

Aguirre, G., Alligood, J., O'Brien, P. & Buyukmihci, N. (1982) Pathogenesis of progressive rod-cone degeneration in miniature poodles. *Investigative Ophthalmology & Visual Science*, 23(5), 610–630.

Aguirre, G.D., Acland, G.M., Maude, M.B. & Anderson, R.E. (1997) Diets enriched in docosahexaenoic acid fail to correct progressive rod-cone degeneration (prcd) phenotype. *Investigative Ophthalmology & Visual Science*, 38(11), 2387–2407.

Allon, G., Mann, I., Remez, L., Sehn, E., Rizel, L., Nevet, M.J. et al. (2019) PRCD is concentrated at the base of photoreceptor outer segments and is involved in outer segment disc formation. *Human Molecular Genetics*, 28(24), 4078–4088.

Berson, E.L., Sandberg, M.A., Rosner, B., Birch, D.G. & Hanson, A.H. (1985) Natural course of retinitis pigmentosa over a three-year interval. *American Journal of Ophthalmology*, 99(3), 240–251.

Branham, K., Samarakoon, L., Audo, I., Ayala, A.R., Cheetham, J.K., Daiger, S.P. et al. (2025) Characterizing the genetic basis for inherited retinal disease: lessons learned from the Foundation Fighting Blindness clinical Consortium's gene poll. *Investigative Ophthalmology & Visual Science*, 66(2), 12.

Calzetti, G., Levy, R.A., Cideciyan, A.V., Garafalo, A.V., Roman, A.J., Sumaroka, A. et al. (2018) Efficacy outcome measures for clinical trials of USH2A caused by the common c.2299delG mutation. *American Journal of Ophthalmology*, 193, 114–129.

Day, A.C., Donachie, P.H., Sparrow, J.M., Johnston, R.L. & Royal College of Ophthalmologists' National Ophthalmology Database. (2015) The Royal College of ophthalmologists' National Ophthalmology Database study of cataract surgery: report 1, visual outcomes and complications. *Eye*, 29(4), 552–560.

den Dunnen, J.T., Dalgleish, R., Maglott, D.R., Hart, R.K., Greenblatt, M.S., McGowan-Jordan, J. et al. (2016) HGVS recommendations for the description of sequence variants: 2016 update. *Human Mutation*, 37(6), 564–569.

Dufour, V.L., Sato, Y., Sumaroka, A., Sudharsan, R., Banin, E., Yu, Y. et al. (2026) PRCD-associated retinitis pigmentosa in dogs and humans. *Experimental Eye Research*, 269, 111045.

Freeman, P.J., Hart, R.K., Gretton, L.J., Brookes, A.J. & Dalgleish, R. (2018) VariantValidator: accurate validation, mapping, and formatting of sequence variation descriptions. *Human Mutation*, 39(1), 61–68.

Fu, Q., Wang, F., Wang, H., Xu, F., Zaneveld, J.E., Ren, H. et al. (2013) Next-generation sequencing-based molecular diagnosis of a Chinese patient cohort with autosomal recessive retinitis pigmentosa. *Investigative Ophthalmology & Visual Science*, 54(6), 4158–4166.

Hanany, M., Rivolta, C. & Sharon, D. (2020) Worldwide carrier frequency and genetic prevalence of autosomal recessive inherited retinal diseases. *Proceedings of the National Academy of Sciences of the United States of America*, 117(5), 2710–2716.

Huang, W.C., Wright, A.F., Roman, A.J., Cideciyan, A.V., Manson, F.D., Gewaily, D.Y. et al. (2012) RPGR-associated retinal degeneration in human X-linked RP and a murine model. *Investigative Ophthalmology & Visual Science*, 53(9), 5594–5608.

Jaganathan, K., Kyriazopoulou Panagiotopoulou, S., McRae, J.F., Darbandi, S.F., Knowles, D., Li, Y.I. et al. (2019) Predicting splicing from primary sequence with deep learning. *Cell*, 176(3), 535–548.e24.

Karczewski, K.J., Francioli, L.C., Tiao, G., Cummings, B.B., Alföldi, J., Wang, Q. et al. (2020) The mutational constraint spectrum quantified from variation in 141,456 humans. *Nature*, 581(7809), 434–443.

Koyanagi, Y., Akiyama, M., Nishiguchi, K.M., Momozawa, Y., Kamatani, Y., Takata, S. et al. (2019) Genetic characteristics of retinitis pigmentosa in 1204 Japanese patients. *Journal of Medical Genetics*, 56(10), 662–670.

Landrum, M.J., Lee, J.M., Benson, M., Brown, G., Chao, C., Chitipiralla, S. et al. (2016) ClinVar: public archive of interpretations of clinically relevant variants. *Nucleic Acids Research*, 44(D1), D862–D868.

McGuigan, D.B., Heon, E., Cideciyan, A.V., Ratnapriya, R., Lu, M., Sumaroka, A. et al. (2017) EYS mutations causing autosomal recessive retinitis pigmentosa: changes of retinal structure and function with disease progression. *Genes (Basel)*, 8(7), 178.

Midgley, N., Rebello, G., Holtes, L.K., Ramesar, R. & Roberts, L. (2024) Screening of inherited retinal disease patients in a low-resource setting using an augmented next-generation sequencing panel. *Molecular Genetics & Genomic Medicine*, 12(12), e70046.

Motipally, S.I., Kolson, D.R., Guan, T. & Kolandaivelu, S. (2024) Aberrant lipid accumulation and retinal pigment epithelium dysfunction in PRCD-deficient mice. *Experimental Eye Research*, 246, 110016.

Nevet, M.J., Shalev, S.A., Zlotogora, J., Mazzawi, N. & Ben-Yosef, T. (2010) Identification of a prevalent founder mutation in an Israeli Muslim Arab village confirms the role of PRCD in the aetiology of retinitis pigmentosa in humans. *Journal of Medical Genetics*, 47(8), 533–537.

Pach, J., Kohl, S., Gekeler, F. & Zobor, D. (2013) Identification of a novel mutation in the PRCD gene causing autosomal recessive retinitis pigmentosa in a Turkish family. *Molecular Vision*, 19, 1350–1355.

Park, S.A., Rhodes, J., Iwabe, S., Ying, G.S., Pan, W., Huang, J. et al. (2022) Quantitative and qualitative characterization of retinal dystrophies in canine models of inherited retinal diseases using spectral domain optical coherence tomography (SD-OCT). *Experimental Eye Research*, 220, 109106.

Peng, X., Wang, X., Wang, Y., Ten, W., Lin, Q. & Zhou, X. (2025) Novel progressive rod-cone degeneration mutation causes retinitis pigmentosa. *Experimental Eye Research*, 254, 110276.

Perez-Carro, R., Corton, M., Sánchez-Navarro, I., Zurita, O., Sanchez-Bolivar, N., Sánchez-Alcudia, R. et al. (2016) Panel-based NGS reveals novel pathogenic mutations in autosomal recessive retinitis pigmentosa. *Scientific Reports*, 6, 19531.

Peter, V.G., Kaminska, K., Santos, C., Quinodoz, M., Cancellieri, F., Cisarova, K. et al. (2023) The first genetic landscape of inherited retinal dystrophies in Portuguese patients identifies recurrent homozygous mutations as a frequent cause of pathogenesis. *PNAS Nexus*, 2(3), pgad043.

Remez, L., Zobor, D., Kohl, S. & Ben-Yosef, T. (2014) The progressive rod-cone degeneration (PRCD) protein is secreted through the conventional ER/Golgi-dependent pathway. *Experimental Eye Research*, 125, 217–225.

17553768, 0, Downloaded from https://onlinelibrary.wiley.com/doi/10.1111/aos.70220 by Servicio Murciano De Salud, Wiley Online Library on [27/10/2026]. See the Terms and Conditions (https://onlinelibrary.wiley.com/terms-and-conditions) on Wiley Online Library for rules of use; OA articles are governed by the applicable Creative Commons License

Richards, S., Aziz, N., Bale, S., Bick, D., Das, S., Gastier-Foster, J. et al. (2015) Standards and guidelines for the interpretation of sequence variants: a joint consensus recommendation of the American College of Medical Genetics and Genomics and the Association for Molecular Pathology. *Genetics in Medicine*, 17(5), 405–424.

Rodríguez-Muñoz, A., Aller, E., Jaijo, T., González-García, E., Cabrera-Peset, A., Gallego-Pinazo, R. et al. (2020) Expanding the clinical and molecular heterogeneity of nonsyndromic inherited retinal dystrophies. *The Journal of Molecular Diagnostics*, 22(4), 532–543.

Roman, A.J., Cideciyan, A.V., Schwartz, S.B., Olivares, M.B., Heon, E. & Jacobson, S.G. (2013) Intervisit variability of visual parameters in Leber congenital amaurosis caused by RPE65 mutations. *Investigative Ophthalmology & Visual Science*, 54(2), 1378–1383.

Spencer, W.J., Ding, J.D., Lewis, T.R., Yu, C., Phan, S., Pearring, J.N. et al. (2019) PRCD is essential for high-fidelity photoreceptor disc formation. *Proceedings of the National Academy of Sciences of the United States of America*, 116(26), 13087–13096.

Zahid, S., Peeler, C., Khan, N., Davis, J., Mahmood, M., Heckenlively, J.R. et al. (2014) Digital quantification of Goldmann visual fields (GVFs) as a means for genotype-phenotype comparisons and detection of progression in retinal degenerations. *Advances in Experimental Medicine and Biology*, 801, 131–137.

Zangerl, B., Goldstein, O., Philp, A.R., Lindauer, S.J., Pearce-Kelling, S.E., Mullins, R.F. et al. (2006) Identical mutation in a novel retinal gene causes progressive rod-cone degeneration in dogs and retinitis pigmentosa in humans. *Genomics*, 88(5), 551–563.

SUPPORTING INFORMATION

Additional supporting information can be found online in the Supporting Information section at the end of this article.

How to cite this article: Kostin, V., Kaminska, K., Cattaneo, M., Ambrosini, E., Ayuso, C., Ávila-Fernández, A. et al. (2026) Clinical and molecular features of *PRCD*-associated retinopathy. *Acta Ophthalmologica*, 00, 1–12. Available from: https://doi.org/10.1111/aos.70220

17553768, 0, Downloaded from https://onlinelibrary.wiley.com/doi/10.1111/aos.70220 by Servicio Murciano De Salud, Wiley Online Library on [27/10/2026]. See the Terms and Conditions (https://onlinelibrary.wiley.com/terms-and-conditions) on Wiley Online Library for rules of use; OA articles are governed by the applicable Creative Commons License